JACS
JOURNAL OF THE AMERICAN CHEMICAL SOCIETY

Article

pubs.acs.org/JACS

In Situ Determination of Tacticity, Deactivation, and Kinetics in [*rac*-(C_2H_4(1-Indenyl)$_2$)ZrMe][$B(C_6F_5)_4$] and [Cp_2ZrMe][$B(C_6F_5)_4$]-Catalyzed Polymerization of 1-Hexene Using ^{13}C Hyperpolarized NMR

Chia-Hsiu Chen, Wei-Chun Shih, and Christian Hilty*

Department of Chemistry, Texas A&M University, 3255 TAMU, College Station, Texas 77843-3255, United States

Supporting Information

ABSTRACT: The stereochemistry, kinetics, and mechanism of olefin polymerization catalyzed by a set of zirconium-based metallocenes was studied by NMR using dissolution dynamic nuclear polarization (DNP). Hyperpolarized 1-hexene was polymerized in situ with a C_2 symmetric catalyst, [(EBI)ZrMe]-[$B(C_6F_5)_4$] (EBI = *rac*-(C_2H_4(1-indenyl)$_2$)), and a C_{2v} symmetric catalyst, [($Cp)_2$ZrMe][$B(C_6F_5)_4$] (Cp = cyclopentadienyl). Hyperpolarized ^{13}C NMR spectra were used to characterize product tacticity following initiation of the reaction. At the same time, a signal gain of 3 orders of magnitude from ^{13}C hyperpolarization enabled the real time observation of catalyst-polymeryl species and deactivation products, such as vinylidene and a Zr-allyl complex. The compounds appearing in the reaction provide evidence for the existence of β-hydride elimination and formation of a dormant site via a methane-generating mechanism. The presence of a deactivating mechanism was incorporated in a model used to determine kinetic parameters of the reaction. On this basis, rate constants were measured between 0.8 and 6.7 mol % of catalyst. The concentration dependence of the rate constants obtained indicates a second-order process for polymerization concomitant with a first-order process for deactivation. The simultaneous observation of both processes in the time evolution of ^{13}C NMR signals over the course of several seconds underlines the utility of hyperpolarized NMR for quantifying early events in polymerization reactions.

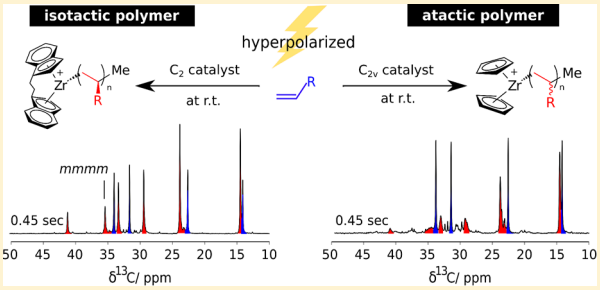

INTRODUCTION

The physical properties of widely used plastics synthesized by olefin polymerization are modulated by the local structure of monomer linkage. Owing to the widespread application of these materials, a precise understanding of the relationship between synthesis and properties of the final product is of high relevance. Metallocene catalysts are known for their tunability toward synthesizing polyolefins with different stereostructures, which is achieved by modifying the symmetry of the ligand (L) on an active catalyst, [$L_2MR^+X^-$].[1−3] Polymerization takes place when the anion (X^-) is displaced by the incoming alkene. During the polymerization reaction, the active species exists in a complicated dynamic equilibrium with the counteranion, solvent, and probably other metal alkyl species.[1−4] Although metallocene-catalyzed polymerization is efficient, it is subject to a decrease in catalytic activity through a number of side reactions, which vary depending on the type of ligand used.[1−3] Common side reactions include 2,1-misinsertion and β-hydride elimination.[2,5−7] Recently, evidence was found for a dormant species, a Zr-allyl complex, which can be generated following β-hydride elimination. This complex may hinder propagation of the polymerization.[2,8−10] Such species are present in small amounts during the reaction and can undergo fast exchange between different coordinated structures and, hence, have in the past been observed using ^{1}H NMR at low temperature.[8,11−13]

Here, we report a comprehensive characterization of the tacticity, kinetics, and mechanisms of deactivation of two metallocene catalysts for olefin polymerization, [(EBI)ZrMe]-[$B(C_6F_5)_4$] and [Cp_2ZrMe][$B(C_6F_5)_4$], using highly sensitive *in situ* ^{13}C NMR. Dissolution dynamic nuclear polarization (DNP),[14] a hyperpolarization technique to enhance NMR signal intensity by several orders of magnitude in a single scan, permits detection of analytes of submillimolar concentration and to follow a chemical reaction in real time within a time frame of seconds.[15−18] Using this technique, it becomes possible to observe the relevant species under room temperature reaction conditions, while making use of the large ^{13}C chemical shift dispersion for chemical identification. At the same time, the rate constants can be calculated by measuring the time evolution of signals stemming from the monomer, in the presence of the two different catalysts.

RESULTS AND DISCUSSION

Time-Resolved Hyperpolarized NMR Spectra. For the metallocene-catalyzed polymerization reactions, 1-hexene was chosen as the monomer. Signal enhancements of >2000 were obtained for this molecule, when compared to single-scan ^{13}C

Received: April 29, 2015
Published: May 11, 2015

DOI: 10.1021/jacs.5b04479
J. Am. Chem. Soc. 2015, 137, 6965−6971

spectra acquired without hyperpolarization in a 9.4 T NMR magnet. This signal gain was sufficient to carry out NMR spectroscopy at natural ^{13}C isotope abundance. In order to allow the observation of catalyst-polymeryl species, a variable amount of catalyst between 0.8−6.7 mol % was used. During the observation window of 12.8 s, a short chain polymer representative of the early stage of the polymerization reaction is obtained. Figure 1a,b shows the time evolution of ^{13}C NMR signals obtained from 1-hexene in the presence of [(EBI)-ZrMe][$B(C_6F_5)_4$] or [Cp_2ZrMe][$B(C_6F_5)_4$], respectively. The strongest observed signals in these spectra stem from a hyperpolarized monomer. Additionally, significant oligomer signals can be identified in the first hyperpolarized ^{13}C spectrum obtained 0.45 s after mixing of the monomer with the catalyst. A hyperpolarized ^{1}H coupled ^{13}C spectrum of the [(EBI)ZrMe][$B(C_6F_5)_4$] catalzyed reaction further shows the expected multiplet patterns in peaks between 14 and 41 ppm, confirming oligomer formation (Figure S3).

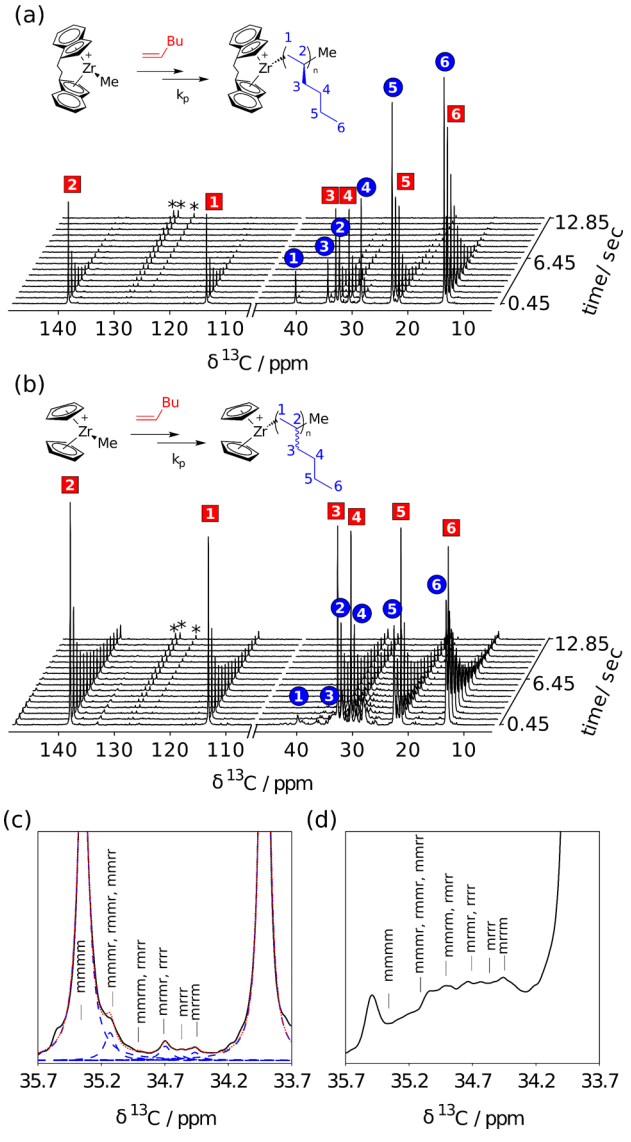

Figure 1. Regions from hyperpolarized ^{13}C NMR spectra acquired during the polymerization of 1-hexene in toluene, at 298 K, using 6.7 mol % of (a,c) [(EBI)ZrMe][$B(C_6F_5)_4$] and (b,d) [Cp_2ZrMe][$B(C_6F_5)_4$]. Numbers in square boxes indicate signals from 1-hexene, and numbers in circles indicate polymer signals. Signals from toluene are designated with *. The anion, $B(C_6F_5)_4^-$, is not shown in the reaction scheme. (c) and (d) are enlarged views of C3 signals of poly(-1-hexene) from the time points at 0.45 s from (a) and (b). Pentad chemical shifts are labeled.[19] The red and blue dotted lines are results from Lorentzian line shape fitting.

Since the ^{13}C chemical shifts in the polymer are sensitive to the adjacent chemical structure, contributions to the signal from different elements of tacticity can be calculated from ^{13}C NMR.[2,19,20] An enlarged view of the spectral region containing the C3 signal from the hyperpolarized experiment is shown in Figure 1c,d. Under the assumption that spin−lattice relaxation affects the C3 atom in all pentads equally, the signal intensity of each peak in the hyperpolarized spectrum is proportional to the concentration of the respective isomer. For the catalyst [(EBI)ZrMe][$B(C_6F_5)_4$], from the data in Figure 1 and three additional data sets, the relative intensity of the isotactic pentad mmmm was calculated to be 86−89% (Table 1) on the basis of the chemical shift assignments from ref 19. Values for other pentads are given in Table S1. The catalytic environment of [(EBI)ZrMe][$B(C_6F_5)_4$], with C_2 symmetry in the ansa-metallocene, is expected to give rise to a high contribution from the isotactic form.[19,20] For comparison, spectra of the products of the corresponding quenched reaction measured without hyperpolarization yielded a similar contribution of 88% mmmm (Table S1 and Figure S2). For polymers of short chain length, different chemical shifts from terminal units can potentially change the apparent contribution from isotacticity in both experiments. A polymer produced in a glovebox using a smaller amount of catalyst to obtain a longer chain length, however, also yielded an isotacticity of 85%. Therefore, under the present conditions, terminal effects do not appear to be dominant. For comparison, in the reaction with a catalytic environment of C_{2v} symmetry ([Cp_2ZrMe][$B(C_6F_5)_4$], Figure 1d) a broader distribution of polymer signals is observed. This distribution is a characteristic feature of atactic polymers due to the irregular sequence of side chain arrangements.[21,22]

Observation of Minor Species in Hyperpolarized Spectra. A closer viewing of the spectra from the *in situ* reaction reveals small signals in addition to those from a monomer or oligomer, which *prima facie* may stem from reaction intermediates or side products (Figure 2 and the inset in Figure S1). Commonly occurring side products are vinylidene-terminated polymer chains, which can form through *β*-hydride elimination.[2,5−7] ^{1}H NMR spectra acquired after the hyperpolarized experiment reveal the existence of unsaturated olefin species in the range of 4.1−6.3 ppm (Figure 3). Due to the presence of chemical shifts from the catalyst in the same spectral region (Figure 3a), the identification of signals in ^{13}C NMR would however, be preferred. In particular, the quaternary carbon of the vinylidene species should be favorable for observation by dissolution DNP, since its long T_1 relaxation time leads to reduced signal attenuation during the experiment. Hyperpolarized ^{13}C NMR spectra acquired without ^{1}H decoupling indeed show two sets of singlet peaks stemming from carbon atoms not bonded to protons, at 148.8 and 173.3 ppm with [(EBI)ZrMe][$B(C_6F_5)_4$] and at 148.8 and 166.8 ppm with [Cp_2ZrMe][$B(C_6F_5)_4$].

The identity of the atoms giving rise to these peaks can be elucidated by an experiment designed to correlate chemical shifts between reactant and product species. This type of experiment, similar to exchange spectroscopy but applied to a nonreversible chemical reaction, is a unique option in the dissolution DNP experiment.[18,23] Such correlation experiments

DOI: 10.1021/jacs.5b04479
J. Am. Chem. Soc. 2015, 137, 6965−6971

Table 1. Experimental Parameters and Rate Constants Obtained from Metallocene-Catalyzed 1-Hexene Polymerization in Toluene at 298 K[a]

entry	ligand	[Zr] (mM)	[Zr] (mol %)	$k_{p(obs)}$ (s^{-1})	k_d (s^{-1})	k_p (M^{-1} s^{-1})	r_p (s^{-1})	isotacticity (%)
1	EBI	19	6.7	0.56	0.15	29	0.90	86
2	EBI	19	6.7	0.36	0.13	19	1.01	88
3	EBI	10	3.4	0.62	0.14	65	1.08	88
4	EBI	10	3.4	0.65	0.12	68	1.04	87
5	EBI	5	1.7	0.30	0.10	63	1.06	86
6	EBI	5	1.7	0.30	0.08	63	1.02	89
7	EBI	2	0.8	0.08	0.13	34	0.98	N.A.
8	EBI	2	0.8	0.08	0.10	34	0.90	N.A.
9	Cp_2	19	6.7	1.73	0.90	97	0.88	N.A.
10	Cp_2	19	6.7	1.85	0.90	91	0.90	N.A.
11	Cp_2	10	3.4	0.97	0.93	102	0.94	N.A.
12	Cp_2	10	3.4	0.88	0.87	93	0.93	N.A.
13	Cp_2	5	1.7	0.43	0.88	91	0.98	N.A.
14	Cp_2	5	1.7	0.51	0.81	107	1.00	N.A.
15	Cp_2	2	0.8	0.03	0.99	13	0.87	N.A.
16	Cp_2	2	0.8	0.04	0.80	17	1.02	N.A.

[a]Rate constants were determined from the experimental data using the kinetic model described in the text. Isotacticity was determined from Lorentzian lineshape fitting. [1-hexene] = 0.283 M was determined from a conventional ^{1}H NMR spectrum without the addition of catalysts. Values of $k_{p(obs)}$ and k_d are obtained using three set of monomer relaxation (Table S2). Standard deviations of $k_{p(obs)}$ and k_d determined from three sets of $r_M + \lambda$ are shown in Figure 5.

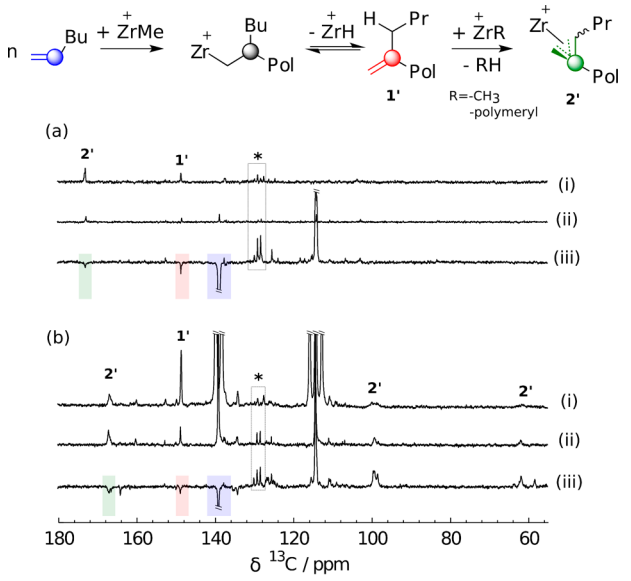

Figure 2. Spectra used for identification of different species in the reactions using (a) [(EBI)ZrMe][$B(C_6F_5)_4$] and (b) [Cp_2ZrMe][$B(C_6F_5)_4$], respectively. Both panels contain ^{13}C hyperpolarized spectra with *J*-coupling to ^{1}H (i), ^{1}H decoupled ^{13}C hyperpolarized spectra (ii), and ^{13}C hyperpolarized spectra with selective inversion of the C2 resonance of 1-hexene at the beginning of the reaction (iii). Peaks denoted with **1′** are assigned to vinylidene, and those with **2′** are assigned to the Zr-allyl complex. Signals from toluene are designated with *.

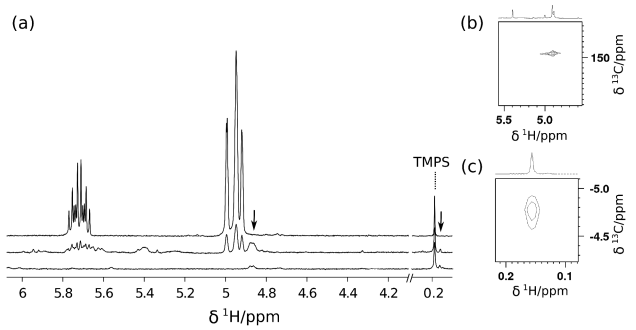

Figure 3. (a) Region of ^{1}H NMR spectra of 1-hexene polymerization acquired after hyperpolarized measurement without catalyst (top) or with [Cp_2ZrMe][$B(C_6F_5)_4$] (middle) and [(EBI)ZrMe][$B(C_6F_5)_4$] (bottom). Trimethylphenylsilane (TMPS) was used as internal standard. Arrows indicate peaks of interest, and the related cross peaks are shown in (b) [^{13}C,^{1}H]-HMBC spectrum from quenched 1-hexene polymerization catalyzed by [(EBI)ZrMe][$B(C_6F_5)_4$] and (c) [^{13}C,^{1}H]-HSQC spectrum of [Cp_2ZrMe][$B(C_6F_5)_4$]-catalyzed 1-hexene polymerization prepared directly in the glovebox.

were performed by injecting the hyperpolarized monomer into the NMR spectrometer, applying a selective inversion pulse on a peak of interest from the reactant, admixing the catalyst using a syringe pump, and acquiring a series of NMR spectra (see Supporting Information section S2 and Scheme S1). In the spectra obtained with inversion of the C2 signal of the monomer, all four of the above identified peaks were inverted, indicating that they originate from this atom. As the signals at 148.8 ppm are identical in the spectra with either of the two catalysts, they likely stem from the vinylidene group[24−26] (**1′** in Figure 2), which is not associated with the catalyst. Correlations to ^{1}H chemical shifts at 4.87 and 4.89 ppm in a non-hyperpolarized heteronuclear multibond correlation spectrum ([^{13}C,^{1}H]-HMBC) of the quenched product further support the identification of this species (Figures 3b and S3).

The signals at 173.3 and 166.8 ppm, which are specific to the catalyst type, likely stem from a Zr-allyl complex (**2′**), which has been described,[8,11−13] but to our knowledge not previously been observed by NMR under typical reaction conditions at room temperature. A similar chemical shift of 162 ppm was reported for the quaternary carbon of [$Cp_2Zr^+(\eta^3$-CH_2C-$(CH_2R)CH_2)$], a model complex stable at 0 °C.[11] Additional signals observed in the DNP spectra, also indicated in Figure 2b, appear to support the existence of the Zr-allyl complex in the polymerization reaction. These chemical shifts are within 7 ppm of the reported chemical shifts of [$Cp_2Zr^+(\eta^3$-CH_2C-

DOI: 10.1021/jacs.5b04479
J. Am. Chem. Soc. 2015, 137, 6965−6971

(Me)CHR)] at 57 ppm (allyl CH_2), 106 ppm (allyl CH) or $[Cp_2Zr^+(\eta^3\text{-}CH_2C(CH_2R)CH_2)]$ at 67 and 68 ppm (allyl CH_2).[11] The Zr-allyl signal (allyl CH) from $[(SBI)Zr\text{-}(CH_2SiMe_3)][B(C_6F_5)_4]$ (SBI = *rac*-$Me_2Si(indenyl)_2$) has been observed at 80 and 84 ppm by Landis et al.[8] by using a $^1H-^{13}C$ HSQC and 1-^{13}C labeled 1-hexene at −40 °C. The hyperpolarized spectrum in Figure S1 also reveals a similar chemical shift at 83.6 ppm.

The existence of noncoordinated vinylidene during the polymerization suggests that the Zr-allyl complex was generated via the previously proposed mechanism, where the Zr-polymeryl complex undergoes β-hydride elimination to generate a vinylidene-terminated polymer, which further recoordinates with the active catalyst, a Zr-methyl cation, to form a Zr-allyl complex and results in the release of methane.[8] A signal at 0.16 ppm (^1H)/−4.8 ppm (^{13}C) in a non-hyperpolarized $[^{13}C,^1H]$-HSQC spectrum of the product from a reaction performed in the glovebox was assigned as methane and further supports the presence of this mechanism (Figures 3c and S4).[1−3]

Kinetic Analysis of Hyperpolarized NMR Signals. The Zr-allyl complex is considered a dormant species with low activity toward olefin insertion and low reinitiation probability.[2,8−10] Formation of this complex can be considered as a deactivation mechanism for the polymerization reaction. Kinetic rate constants pertaining to polymerization, as well as to deactivation by this or other mechanisms, can be determined from the time-resolved DNP-NMR spectra. In the absence of catalyst deactivation, such as in a living polymerization (Scheme 1a), the monomer consumption follows a pseudo-first-order rate law. Considering the spin up and spin down concentration, the monomer signal evolution in the hyperpolarized NMR experiment can be described by[16,18]

$$\frac{d}{dt}S_M = -(r_M + \lambda)S_M - k_{p(obs)}S_M \quad (1)$$

The first term originates from the intrinsic monomer spin−lattice relaxation, r_M, and the signal loss due to the application of small flip angle pulses ($\lambda = -\ln(\cos\alpha)/\Delta t$, with Δt as the time delay between scans and α as the flip angle of radio frequency excitation). The second term is due to the depletion of the monomer signal from the polymerization process by a rate constant, $k_{p(obs)} = k_p[C]_0$. The analytical solution of eq 1 can be written in logarithmic form:

$$\ln(S_M(t)) - \ln(S_M(0)) = -(r_M + \lambda + k_{p(obs)})t \quad (2)$$

The above equation indicates a pseudo-first-order time dependence, characterized by a straight line with slope $r_M + \lambda + k_{p(obs)}$. The data from peak integration in Figure 4 however indicate that the rate constant for monomer consumption is larger at the beginning of the reaction, as evidenced by the nonlinear appearance of the plot of $\ln(S_M)$ against time. Hence, a modified kinetic model (Scheme 1b) is proposed to account for the decreasing catalytic activity. An assumption is made that the catalyst-polymeryl species, CP_i, undergoes a first-order deactivation process, with a rate constant k_d, to yield a terminal species CP_i*. In this case, the time evolution of monomer signal can be described by

$$\frac{d}{dt}S_M = -(r_M + \lambda)S_M - k_{p(obs)}\, e^{-k_d t}S_M \quad (3)$$

where the rate of monomer signal decay is further affected by an exponential factor dependent on k_d. In logarithmic form, the time evolution of hyperpolarized monomer signal in the presence of this deactivation mechanism becomes

$$\ln(S_M(t)) - \ln(S_M(0)) = -(r_M + \lambda)t - (k_{p(obs)}/k_d)(1 - e^{-k_d t}) \quad (4)$$

(see also Supporting Information section S5). This equation fits the hyperpolarized signal more closely than the simple exponential eq 2 supporting the presence of a deactivation mechanism in the present reaction. A comparison of the two data sets in Figure 4 shows a more significant deactivation (larger curvature) in $[Cp_2ZrMe][B(C_6F_5)_4]$. Although kinetic data cannot directly be used to identify the deactivation mechanism, notably this catalyst also gives rise to stronger signals identified as the Zr-allyl complex and vinylidene in the hyperpolarized ^{13}C spectra in Figure 2.

Dependence of Observed Rates on Catalyst Concentration. A series of experiments were performed to determine the influence of catalyst concentration, starting from 0.8 mol %. Representative signals from these experiments are shown in Figure 5a,b. A decrease in catalyst concentration reduces the relative contribution of the second term in eq 4. Hence, the

Scheme 1. Proposed Kinetic Pathways for the 1-Hexene Polymerization[a]

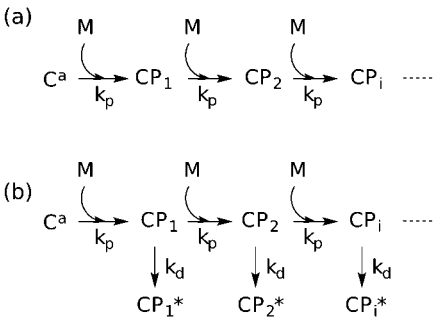

[a](a) Living polymerization. (b) Polymerization with deactivation. C^a is the activated catalyst, CP_i is the catalyst-polymeryl species, and CP_i* is the deactivated catalyst-polymeryl species. k_p and k_d are second- and first-order rate constants, respectively.

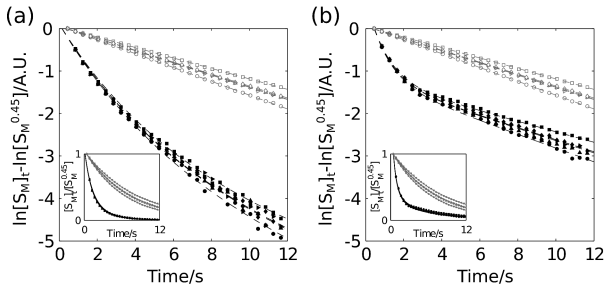

Figure 4. Time evolution of signal integrals (logarithmic scale) of monomer C1 to C5 from hyperpolarized NMR of polymerization reaction catalyzed by (a) $[(EBI)ZrMe][B(C_6F_5)_4]$ and (b) $[Cp_2ZrMe][B(C_6F_5)_4]$ from Figure 1 (filled symbols). In both panels, empty gray symbols are from measurements without the catalyst. The black fitted lines were obtained using eq 4, and the gray fitted lines were obtained using an exponential time dependence. The insets show the integrals on a linear scale.

DOI: 10.1021/jacs.5b04479
J. Am. Chem. Soc. 2015, 137, 6965−6971

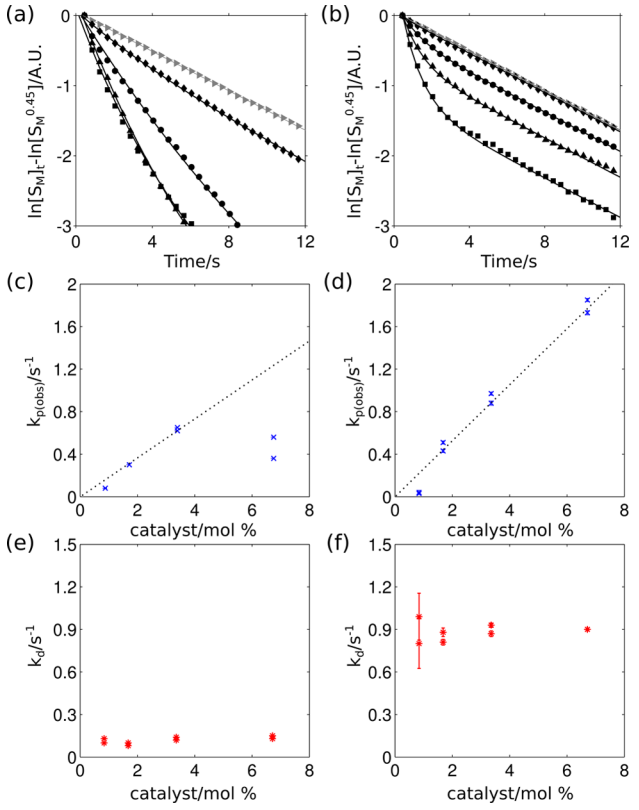

Figure 5. (a,b) Time evolution of signal integrals of C5 and (c–f) rate constants $k_{p(obs)}$ and k_d, determined from hyperpolarized ^{13}C NMR at different catalyst concentrations of (a,c,e) [(EBI)ZrMe][$B(C_6F_5)_4$] and (b,d,f) [Cp_2ZrMe][$B(C_6F_5)_4$]. The $k_{p(obs)}$ and k_d were calculated from the solid lines in (a) and (b), which were obtained using eq 4. Error bars represent the standard deviation from three separate reference sets of $r_M + \lambda$. The dotted line is a linear fit of the $k_{p(obs)}$ with respect to concentration.

signal intensities decrease less rapidly, and the curvature becomes less pronounced. Eventually, the time course of the monomer signal approaches the straight line obtained in the absence of catalyst. This behavior is observed at the catalyst concentration of 0.8 mol %, which is close to the lower limit of the concentration range that can be investigated with this method.

The rate constants calculated from the hyperpolarized ^{13}C NMR data sets at all concentrations are summarized in Table 1. These values were determined by simultaneously fitting all signals from C1 to C5 of the monomer, as shown in Figures 4, S5, and S6 using the parameter $r_M + \lambda$ found from experiments in the absence of catalyst (Table S2).

The concentration dependence of the determined rate constants is plotted in Figure 5c–f. The data points in general follow a linear trend, with a positive slope for $k_{p(obs)}$ indicating a second-order process for the polymerization reaction. At the highest catalyst concentration, 6.7 mol %, the $k_{p(obs)}$ determined using [(EBI)ZrMe][$B(C_6F_5)_4$] fluctuates and falls below the linear trend. We attribute this behavior to low solubility of the activated catalyst in toluene, supported by visual observation of a precipitate, which can lead to an underestimated k_p value. At the lowest catalyst concentration of 0.8 mol % of [Cp_2ZrMe][$B(C_6F_5)_4$], the time course of the signal approaches that without catalyst. This results in a larger variation of the $k_{p(obs)}$ and k_d calculated on the basis of three independently measured values for $r_M + \lambda$, as shown in Figure 5d,f.

The averaged k_p from the linear fit is 65 M^{-1} s^{-1} for [(EBI)ZrMe][$B(C_6F_5)_4$] and 95 M^{-1} s^{-1} for [Cp_2ZrMe][$B(C_6F_5)_4$]. The rate constant k_p is 4 times higher than that observed in a study by Christianson et al.,[27] which was obtained using stopped-flow NMR of 1-hexene polymerization with nonhyperpolarized ^1H NMR. The higher k_p in the present study may be due to the use of $[B(C_6F_5)_4]^-$ as a weaker counteranion, which is believed to increase the reactivity.[4] In contrast to the rate constant for polymerization, the observed rate constant for the deactivation process, k_d, is independent of catalyst concentration. This property indicates that the dominant deactivation mechanism under these conditions is a first-order reaction and supports the idea that an extrapolation to even lower catalyst concentrations may be valid. Concomitantly with the curvature in the time course of monomer signal intensities due to deactivation, signals pertaining to Zr-allyl species are observed in spectra acquired after a single 90° pulse at all but the lowest catalyst concentrations (Figure S7).

A comparison of rate constants between two catalysts show a smaller k_p value for the ansa-metallocene [(EBI)ZrMe][$B(C_6F_5)_4$] to [Cp_2ZrMe][$B(C_6F_5)_4$], despite the larger access space to the coordination site of the former. While for a monomer such as propylene the ansa-metallocene catalyst would be expected to be more active, the interaction of the ligands on the catalyst with monomers can significantly influence the rate of catalysis.[28] For 1-hexene, Soga et al. found a lower activity in $Et(IndH_4)_2ZrCl_2$ compared to Cp_2ZrCl_2.[29] These two catalysts are similar in structure to those employed here and give rise to the same trend as seen in Figure 5c,d.

Observed Polymer Signals. The proposed model also allows calculation of the time dependence of signals from the polymer. Here, the relaxation rates of the polymer and deactivated polymeryl species are assumed to be identical and are denoted as r_P. The rate expression of the signal intensity of polymer can be described as

$$\frac{d}{dt}S_P = -(r_P + \lambda)S_P + k_{p(obs)}\, e^{-k_d t} S_M \quad (5)$$

(see also Supporting Information section S5). This time dependence was further examined with a numerical calculation, using $r_M + \lambda$ from Table S2, and $k_{p(obs)}$, k_d, $S_M(0)$ determined from the previous fitting step (eq 4). The curves found by fitting with the remaining unknowns, r_P and $S_P(0)$, are shown in Figures 6 and S8. As may be expected, the ratio of S_M/S_P at t = 0.45, i.e. the first acquired data point, is approximately proportional to the catalyst amount (Figure 6b,d), except for the highest concentration of [(EBI)ZrMe][$B(C_6F_5)_4$], which deviates due to solubility. Further, the obtained r_P values (Table 1) are within the expected range for the polymer size obtained, supporting the validity of the numerical values.

CONCLUSION

In summary, dissolution DNP-NMR permitted the simultaneous characterization of product tacticity, measurement of rate constants, and identification of deactivation processes in metallocene-catalyzed 1-hexene polymerization reactions. The stopped-flow DNP-NMR apparatus provided a sufficiently inert environment to enable study of the reactions with an air and moisture sensitive organometallic catalyst. Hyperpolarized 1-

DOI: 10.1021/jacs.5b04479
J. Am. Chem. Soc. 2015, 137, 6965–6971

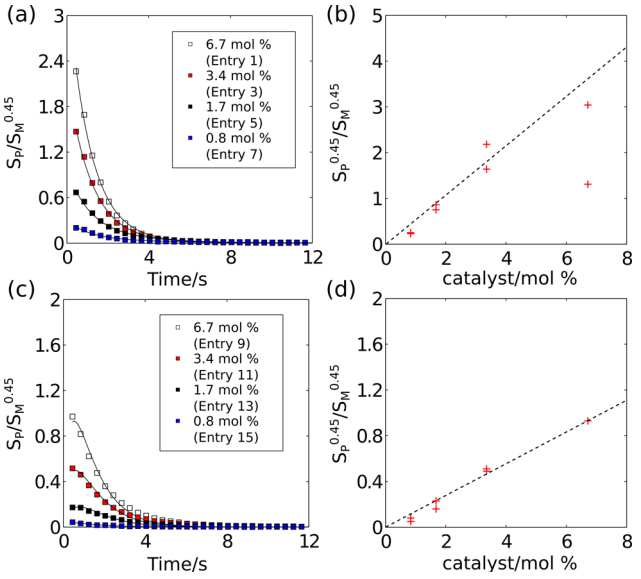

Figure 6. (a,c) Time evolution of signal integrals of polymer C5 from hyperpolarized ^{13}C NMR measurements. Solid lines are from the numerical fit based on eq 5. (b,d) Calculated ratio of polymer signal to monomer signal, S_P/S_M, at t = 0.45 s. (a) and (b) are from [(EBI)ZrMe][$B(C_6F_5)_4$]-catalyzed and (c) and (d) from [Cp_2ZrMe]-[$B(C_6F_5)_4$]-catalyzed 1-hexene polymerization.

hexene, at natural isotope abundance, was used to detect the influence of a chiral and an achiral catalytic environment on the polymerization, without the need for postreaction quenching and separation processes. Reactive species such as a Zr-allyl complex difficult to capture under ambient temperature were readily detectable in the real-time NMR spectra. A quantitative model yielded rate constants for polymerization in the presence of a deactivation process. The dissolution DNP-NMR method is likely applicable to a broad range of polymerization reactions and may provide valuable information for the design of catalysts yielding polymers with specific properties.

EXPERIMENTAL SECTION

Polymerization Reactions. Bis(cyclopentadienyl)dimethylzirconium(IV) and trityltetra(pentafluorophenyl)borate (cocatalyst) were purchased from Strem Chemicals, Inc., Newburyport, MA. *rac*-Ethylenebis(indenyl)dimethylzirconium(IV) was prepared according to literature procedures.[30] Toluene and fluorobenzene were dried over and distilled from NaK/Ph_2CO/18-crown-6 and stored in an Ar-filled glovebox. 1-Hexene was dried over and distilled from NaK/18-crown-6. All polymerization experiments were performed with 1.1 equiv of a cocatalyst and 1 mM trimethylphenylsilane (TMPS) as an internal standard. The catalyst activation was examined by the signal of [CPh_3Me] in ^1H NMR (δ 2.03, Me). Bridge complexes were also found in the spectrum at 298 K; those structures were omitted for clarity. Before the dissolution of the hyperpolarized sample, the activated catalytic ion pair was prepared by mixing the catalyst and the cocatalyst in 50 μL of fluorobenzene in an Ar-filled glovebox with subsequent transfer to a 5 mm NMR tube. Before installation of the NMR tube into the NMR instrument, the transfer line was purged with Ar gas to avoid moisture and oxygen from room air. After the hyperpolarized NMR measurement, the polymerization reaction was quenched with acidified methanol. The volatiles were removed by a rotary evaporator, and the generated polymer was extracted using a hexane and methanol mixture.

Dynamic Nuclear Polarization. A sample of 5 mM α,γ-bis-diphenylene-β-phenylallyl (BDPA; Sigma-Aldrich, St. Louis, MO; concentration is chosen for solubility) in 50 μL of neat 1-hexene (Alfa Aesar, Ward Hill, MA) was hyperpolarizd in a HyperSense system (Oxford Instruments, Abingdon, U.K.) at 1.4 K under the irradiation of microwaves at $\omega_e - \omega_N$ = 93.965 GHz and a power of 60 mW. After 4 h, the hyperpolarized sample was dissolved in 4 mL of hot toluene 800 kPa(g) and transferred into the rapid injection system by He gas.[31] A photodiode sensed the arrival of the hyperpolarized sample, at which point the hyperpolarized sample was rapidly injected by Ar gas into the NMR tube where the activated catalyst was preloaded (preloading was done in a glovebox before the experiment). The injection was accomplished with a forward pressure of 214 psi applied against a back pressure of 150 psi for 355 ms, followed by stabilization for 400 ms. The time t = 0 was defined as the midpoint between start and end of injection and mixing, and the first data point was acquired at t = 0.45 s. The final temperature was 298 K. Injection parameters were optimized using a ^{19}F pulsed field gradient experiment to ensure a homogeneous mixture,[17] and a Diels–Alder reaction was used as a stopped-flow control experiment.[18]

NMR Spectroscopy. The hyperpolarized ^{13}C NMR spectra were acquired using a Bruker 400 MHz NMR spectrometer equipped with a broad-band probe containing three pulse field gradients (Bruker Biospin, Billerica, MA) at a temperature of 298 K. The time evolution NMR signal is measured with a pulse sequence, $[G_z\text{-}\alpha_x\text{-acquire}]_{x32}$. The NMR measurement was triggered after the hyperpolarized 1-hexene was delivered to the NMR tube. For each experiment, a data set with a total acquisition time of 12.8 s includes 32 transients separated by 400 ms. A randomized pulsed field gradient, G_z (35.5 G/cm, 1 ms), was applied to remove the residual coherence from the previous scan. A small flip angle, α = 16.65°, with pulse strength γB_1 = 31.25 kHz was applied after the G_z. During the acquisition, WALTZ-16 ^1H decoupling was applied with field strength γB_1 = 2.78 kHz. In each scan, 15 924 data points were acquired. The temporal correlation experiment (Figure 2) is measured with a two-step injection process (see Supporting Information section S2) and a single transient pulse sequence, (shaped π)-G_z-(π/2)-acquire. An IBURP2 shaped pulse of flip angle π and 10 ms duration at the resonance frequency of C1 or C2 of 1-hexene was applied. A pulsed field gradient, G_z (35.5 G/cm, 1 ms), and a 90 deg pulse with field strength γB_1 = 31.25 kHz were also applied. During the acquisition, WALTZ-16 ^1H decoupling was applied with field strength γB_1 = 2.78 kHz. The acquisition time was 2.38 s, and 95 964 data points were collected. Nonhyperpolarized ^1H NMR spectra (Figure 3a) were acquired by using 30 degree pulses with field strength γB_1 = 22.87 kHz, an acquisition time of 1 s, and 4 transients. The toluene resonance was saturated with continuous rf irradiation. Chemical shifts were referenced to the solvent resonance of toluene. The chemical shift of toluene was calibrated against tetramethylsilane (TMS) using a separate sample according to the IUPAC recommendations. Trimethylphenylsilane (TMPS) was used as an internal standard. Other nonhyperpolarized NMR spectra (Figures 3bc and S2–S4) were acquired using a 500 MHz NMR spectrometer equipped with a triple resonance TCI cryoprobe with a Z-gradient (Bruker Biospin), at 298 K. The detailed experimental parameters are listed in the Supporting Information.

ASSOCIATED CONTENT

Supporting Information

Methods and additional data. The Supporting Information is available free of charge on the ACS Publications website at DOI: 10.1021/jacs.5b04479.

AUTHOR INFORMATION

Corresponding Author

*chilty@tamu.edu

Notes

The authors declare no competing financial interest.

ACKNOWLEDGMENTS

We thank Prof. Oleg V. Ozerov for giving access to equipment for synthesizing the catalyst and Hsueh-Ying Chen for

DOI: 10.1021/jacs.5b04479
J. Am. Chem. Soc. 2015, 137, 6965–6971

assistance with DNP polarization. Acknowledgment is made to the Donors of the American Chemical Society Petroleum Research Fund for support of this research (Grant 50813-ND7). Support from the National Science Foundation (Grants CHE-0840464 and CHE-0846402) is gratefully acknowledged.

REFERENCES

(1) Coates, G. W. *Chem. Rev.* **2000**, *100*, 1223.
(2) Resconi, L.; Cavallo, L.; Fait, A.; Piemontesi, F. *Chem. Rev.* **2000**, *100*, 1253.
(3) Brintzinger, H. H.; Fischer, D.; Mülhaupt, R.; Rieger, B.; Waymouth, R. M. *Angew. Chem., Int. Ed. Engl.* **1995**, *34*, 1143.
(4) Bochmann, M. *J. Organomet. Chem.* **2004**, *689*, 3982.
(5) Liu, Z.; Somsook, E.; White, C. B.; Rosaaen, K. A.; Landis, C. R. *J. Am. Chem. Soc.* **2001**, *123*, 11193.
(6) Novstrup, K. A.; Travia, N. E.; Medvedev, G. A.; Stanciu, C.; Switzer, J. M.; Thomson, K. T.; Delgass, W. N.; Abu-Omar, M. M.; Caruthers, J. M. *J. Am. Chem. Soc.* **2010**, *132*, 558.
(7) Song, F.; Cannon, R. D.; Bochmann, M. *J. Am. Chem. Soc.* **2003**, *125*, 7641.
(8) Landis, C. R.; Christianson, M. D. *Proc. Natl. Acad. Sci. U.S.A.* **2006**, *103*, 15349.
(9) Al-Humydi, A.; Garrison, J. C.; Mohammed, M.; Youngs, W. J.; Collins, S. *Polyhedron* **2005**, *24*, 1234.
(10) Margl, P. M.; Woo, T. K.; Ziegler, T. *Organometallics* **1998**, *17*, 4997.
(11) Vatamanu, M.; Stojcevic, G.; Baird, M. C. *J. Am. Chem. Soc.* **2008**, *130*, 454.
(12) Vatamanu, M. *Organometallics* **2014**, *33*, 3683.
(13) Sauriol, F.; Wong, E.; Leung, A. M. H.; Donaghue, I. E.; Baird, M. C.; Wondimagegn, T.; Ziegler, T. *Angew. Chem., Int. Ed.* **2009**, *48*, 3342.
(14) Ardenkjaer-Larsen, J. H.; Fridlund, B.; Gram, A.; Hansson, G.; Hansson, L.; Lerche, M. H.; Servin, R.; Thaning, M.; Golman, K. *Proc. Natl. Acad. Sci. U.S.A.* **2003**, *100*, 10158.
(15) Keshari, K. R.; Wilson, D. M. *Chem. Soc. Rev.* **2014**, *43*, 1627.
(16) Lee, Y.; Heo, G. S.; Zeng, H.; Wooley, K. L.; Hilty, C. *J. Am. Chem. Soc.* **2013**, *135*, 4636.
(17) Bowen, S.; Hilty, C. *Angew. Chem., Int. Ed.* **2008**, *47*, 5235.
(18) Zeng, H.; Lee, Y.; Hilty, C. *Anal. Chem.* **2010**, *82*, 8897.
(19) Asakura, T.; Demura, M.; Nishiyama, Y. *Macromolecules* **1991**, *24*, 2334.
(20) Tonelli, A. E. *NMR Spectroscopy and Polymer Microstructure: The Conformational Connection; Methods in Stereochemical Analysis*; Wiley-VCH: New York, 1989.
(21) Subramanyam, U.; Rajamohanan, P. .; Sivaram, S. *Polymer* **2004**, *45*, 4063.
(22) Segal, S.; Goldberg, I.; Kol, M. *Organometallics* **2005**, *24*, 200.
(23) Bowen, S.; Hilty, C. *Anal. Chem.* **2009**, *81*, 4543.
(24) Harvey, B. G.; Meylemans, H. A. *Green Chem.* **2014**, *16*, 770.
(25) Babu, G. N.; Newmark, R. A.; Chien, J. C. W. *Macromolecules* **1994**, *27*, 3383.
(26) Landis, C. R.; Rosaaen, K. A.; Sillars, D. R. *J. Am. Chem. Soc.* **2003**, *125*, 1710.
(27) Christianson, M. D.; Tan, E. H. P.; Landis, C. R. *J. Am. Chem. Soc.* **2010**, *132*, 11461.
(28) Kaminsky, W.; Engehausen, R.; Zoumis, K.; Spaleck, W.; Rohrmann, J. *Makromol. Chem.* **1992**, *193*, 1643.
(29) Soga, K.; Lee, D. H.; Morikawa, Y. *Polymer* **1992**, *33*, 2408.
(30) Camara, J. M.; Petros, R. A.; Norton, J. R. *J. Am. Chem. Soc.* **2011**, *133*, 5263.
(31) Bowen, S.; Hilty, C. *Phys. Chem. Chem. Phys.* **2010**, *12*, 5766.

DOI: 10.1021/jacs.5b04479
J. Am. Chem. Soc. 2015, 137, 6965−6971